Sub-5 nm electron-beam lithography and metrology of poly (methyl methacrylate) using an aberration-corrected scanning transmission electron microscope

Vitor R. Manfrinato[1*], Aaron Stein[1], Lihua Zhang [1], Eric A. Stach[1], and Charles T. Black[1].

[1] Center for Functional Nanomaterials, Brookhaven National Laboratory, NY, USA

*electronic mail: vmanfrinato@bnl.gov

Understanding the ultimate resolution limit of electron-beam lithography (EBL) is a complex challenge due to the many interconnected physical and chemical processes involved.[1] In order to compare distinct exposure processes simultaneously we performed a unified analysis of electron beam exposure of poly (methyl methacrylate) (PMMA) to simultaneously form positive and negative tone resists structures, as well as carbon nanostructures by electron-beam-induced deposition (EBID). The resolution limit of PMMA (both tones) may ultimately be limited by volume plasmons[1] (VPs) and secondary electrons (SEs).[2,3] The resolution limit of EBID has been attributed to SEs[4] and may be indirectly affected by VPs due to their strong attenuation at a surface. We believe a simultaneous analysis of EBL and EBID could provide new insights in understanding each process. For these experiments we used an aberration-corrected scanning transmission electron microscope (STEM) with 0.1 nm probe diameter and 200 keV as the exposure tool. We performed resist metrology using the same STEM – an approach that has not previously been widely explored in the field. STEM metrology provided additional information about the exposure process compared to other methods, because the STEM signal is proportional to the resist thickness.[5] We obtained STEM images of previously exposed areas of PMMA without development, obtaining topographic images as a function of dose. This method of imaging enable the visualization of the exposure process *in situ*, in a similar manner to what has been demonstrated using atomic force microscopy.[6]

Figure 1A shows a set of three structures fabricated simultaneously: PMMA holes, negative-tone PMMA pillars, and carbon dots. Figure 1B-F show fabricated sub-10 nm structures. Figure 2A shows calculated point-spread functions (PSFs) from measurements of STEM images (Fig. 1) for the three distinct exposure modes. We have assumed a simplified energy threshold model for the lithographic development, carbon deposition, and thickness loss. The PSF for carbon-deposition has the largest slope, which may indicates a higher resolution for EBID. The three PMMA PSFs presented similar shape. Figure 2B presents both the negative-tone and thickness-loss PSFs, which show strong agreement. The thickness-loss PSF was acquired at two imaging dosages (6 and 47 electrons/Å^2) to rule out imaging artifacts. We believe this may be a useful technique to directly image the resist exposure. Finally, we will discuss the advantages of simultaneous SEM and STEM metrology of lithographic nanostructures.

1. Manfrinato, V. *et al*. Nano Lett. 14 4406 (2014); **2**. Duan, H. *et al*. JVST B 28 C6C58 (2010); **3**. Rommel, M. *et al*. Microelectron. Eng. 98 202 (2012); **4**. Silvis-Cividjian, N. *et al*. J. Appl. Phys. 98 (2005); **5**. Wall, J. & Hainfeld, J. Ann. Rev. Bio. Biophys. Chem. 15, 355 (1986); **6**. Ocola, L. *et al*. Appl. Phys. Lett. 68 717 (1996).

This research used resources of the Center for Functional Nanomaterials, which is a U.S. DOE Office of Science Facility, at Brookhaven National Laboratory under Contract No. DE-SC0012704.

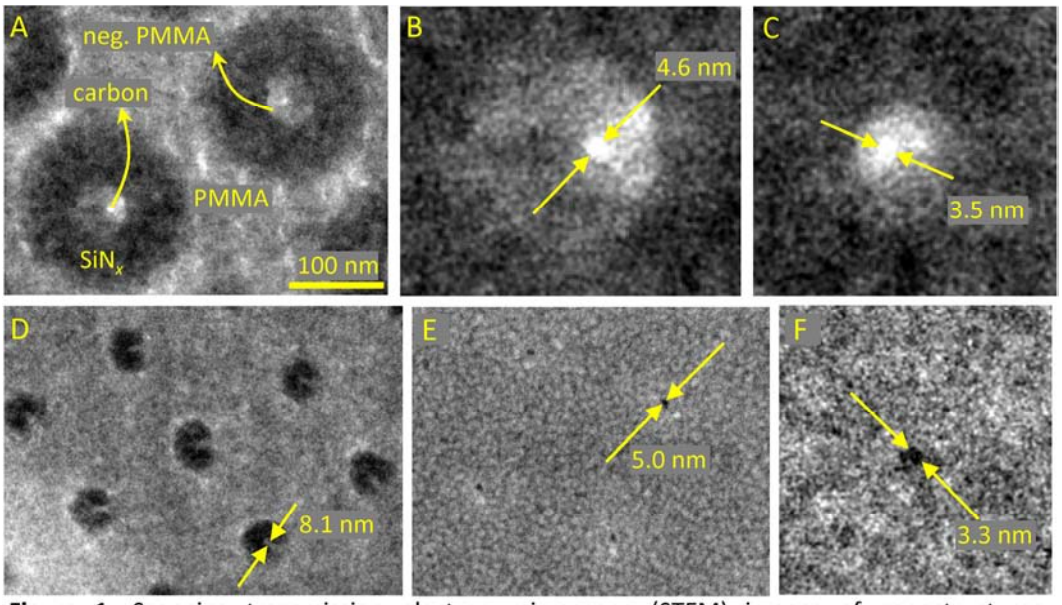

Figure 1. Scanning transmission electron microscope (STEM) images of nanostructures fabricated using STEM electron-beam lithography and STEM induced deposition at 200 keV. All structures were on top of 10-nm-thick SiN_x membrane. **A.** Three circular structures were observed: (1) positive-tone PMMA hole (dark ring); (2) negative-tone PMMA pillar (grey disk); and (3) carbon deposit on top of the PMMA pillar (white dot). The three structures were exposed simultaneously and all were developed in 3:1 IPA:MIBK for 30s at 0°C. **B** and **C**. STEM images of negative tone PMMA pillars and sub-5 nm diameter carbon deposited dots. **D.** STEM image of fallen over PMMA pillars with diameter smaller than 10 nm. **E** and **F**. STEM images of sub-5 nm PMMA holes with Al top coating to improve image contrast and stability.

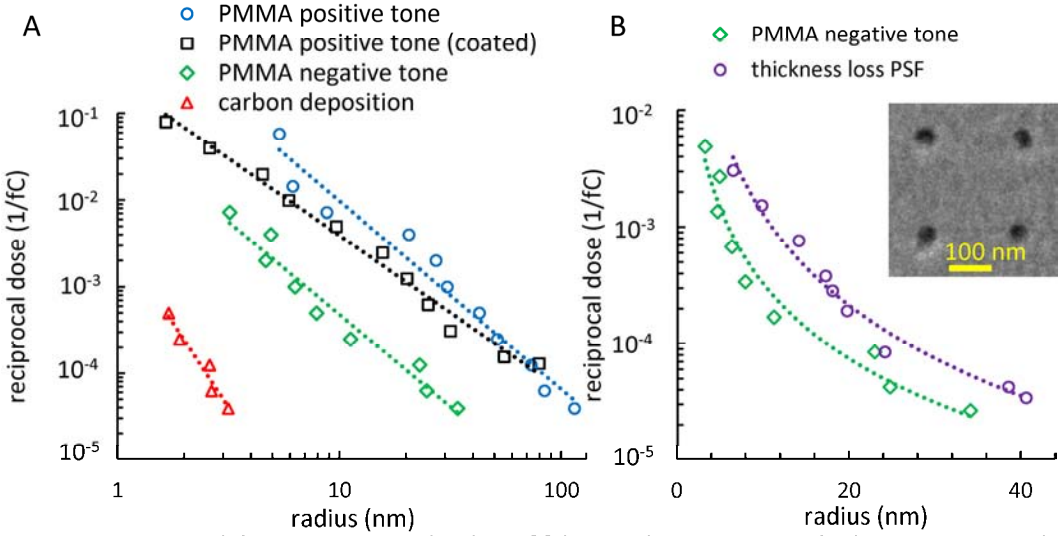

Figure 2. Reciprocal dose *vs.* measured radius of fabricated structures. Each plot is proportional to the point-spread function (PSF), assuming a simplified threshold exposure model for each process. **A.** Red triangles: carbon-deposition PSF. Green diamonds: Negative-tone PMMA PSF. Blue circles: PMMA PSF measured without coating. Black squares: PMMA PSF measured with Al coating. Dotted lines: Fitting with power functions. The carbon-deposition PSF shows the largest slope. The negative-tone PMMA PSF shows slope similar the two measured PMMA PSFs. **B.** Green diamonds: Negative-tone PMMA PSF. Purple circle: Reciprocal dose *vs.* radius of holes created in PMMA without development, def. as thickness-loss PSF. Inset: STEM image of holes created in PMMA after electron irradiation without development. The thickness-loss PSF correlates well with the negative-tone PMMA PSF.